LAWRENCE
LIVERMORE
NATIONAL
LABORATORY

LLNL-JRNL-751782

Modelling the Effect of Divertor Closure on Detachment Onset in DIII-D with the SOLPS code

L. Casali, C. Sang, B. M. Covele, H. Y. Guo, A. L. Moser, C. Samuell

May 23, 2018

Contributions to Plasma Physics

Disclaimer

This document was prepared as an account of work sponsored by an agency of the United States government. Neither the United States government nor Lawrence Livermore National Security, LLC, nor any of their employees makes any warranty, expressed or implied, or assumes any legal liability or responsibility for the accuracy, completeness, or usefulness of any information, apparatus, product, or process disclosed, or represents that its use would not infringe privately owned rights. Reference herein to any specific commercial product, process, or service by trade name, trademark, manufacturer, or otherwise does not necessarily constitute or imply its endorsement, recommendation, or favoring by the United States government or Lawrence Livermore National Security, LLC. The views and opinions of authors expressed herein do not necessarily state or reflect those of the United States government or Lawrence Livermore National Security, LLC, and shall not be used for advertising or product endorsement purposes.

Modelling the effect of divertor closure on detachment onset in DIII-D with the SOLPS code

L. Casali[1*], C. Sang[2], B.M. Covele[3], H.Y. Guo[3], A.L. Moser[3], C. Samuell[4]

[1]*Oak Ridge Associated Universities, Oak Ridge, TN, USA / General Atomics, San Diego, CA, USA*
[2]*Dalian University of Technology, China*
[3]*General Atomics, San Diego, CA, USA*
[4]*Lawrence Livermore National Laboratory, Livermore, CA, USA*

[*]*e-mail contact: casalil@fusion.gat.com*

Abstract

SOLPS modeling has shown that divertor plasma detachment occurs at a lower upstream separatrix density in the more closed DIII-D upper divertor than the open lower divertor demonstrating divertor closure's utility in widening the range of acceptable densities for adequate heat handling. To achieve reduced heat flux and erosion at the plasma facing components, future devices will need to operate in at least partially detached divertor conditions [1]. 2D fluid plasma models coupled to Monte Carlo neutral transport simulations, such as SOLPS, have been widely used to predict the onset of detachment. In modeling the DIII-D discharges the cross-field transport coefficients are constrained to reproduce the experimental upstream profiles. The closed divertor has been modelled with the same input parameters of the open divertor allowing a direct comparison of target conditions in both geometries. SOLPS simulations indicate that higher molecular density correlates strongly with lower electron temperatures. The increased closure of the upper divertor improve the trapping of neutrals thereby reducing the power density deposited at the target and facilitating detachment in agreement with experimental observations.

1. Introduction

The effects of divertor closure in the DIII-D tokamak are investigated with a detailed comparison between experimental measurements and simulated plasma at the detachment onset. Future reactors' divertors will need to operate in some degree of detachment to (1) ensure the divertor target heat load $q_t \leq 10$ MW/m^2, and (2) divertor target plasma temperature: $T_t \leq 5$ eV to suppress erosion [1]. Moreover, Greenwald density fraction, n_e/n_{GW} is currently constrained to ~0.5, for efficient current drive and high performance operation. The detachment process can be characterized by a drop in the particle flux at the target which can be measured as the roll-over of the ion saturation current (J_{sat}) and by electron temperatures below 2 eV. However, detachment currently requires high upstream densities, which are concurrent with degraded core performance, and which make power and current drive more difficult via higher electron collisionality. The combination of highly dissipative divertor with advanced tokamak operation required for future reactors calls for innovative divertor solution. Increased divertor closure and a baffle geometry more aligned along the flux contours are potentially an effective way to optimize power dissipation [2] [3][4].Experimental studies of the effect of divertor closure have been carried out at the DIII-D tokamak and show detachment onset at 20% lower pedestal density in the more closed divertor [5]. Here, the SOLPS code [6] is used to assess the closure effect by modeling the experiments in both the open lower divertor shelf and the more-closed upper divertor. The model shows that the increased closure of the upper divertor improves the trapping of neutrals, thereby reducing the power density deposited at the target and facilitating the detachment process.
The paper is organized as follows: experimental set up and results are given in Section 2, the modelling set up is discussed in Section 3, the results of the modelling are discussed in Section 4, summary and conclusion are in Section 5.

2. Experimental setup and results

Experiments were carried out at DIII-D using two different configurations: the lower single-null (LSN) which is the open configuration on the shelf and the upper single-null (USN) which is the more-closed upper divertor as shown in Figure 1. The nearly identical conditions of the LSN and USN plasmas allowed for a direct comparison of the open and closed divertor. Experiments were performed in H-mode with P_{NBI}=3 MW and I_p=1.4MA, B_t= 2.1T for both configurations. The magnetic geometries were matched as closely as possible, as well as plasma shape, ion $\nabla B \times B$ drift direction, fueling location, triangularity, x-point height. A shot to shot density scan delivered the peak

target J_{sat} as function of pedestal electron density $n_{e,ped}$, as shown in Figure 1, where J_{sat} is measured by the Langmuir probes embedded in the divertor target plates. In-target Langmuir probes in upper and lower divertor enable a direct comparison of the ion saturation current at the target J_{sat}. The roll-over of J_{sat} indicates the detachment onset, which occurs at 20% lower pedestal density in the more-closed divertor. From Figure 2 (right) the J_{sat} roll over in the upper divertor is in the range $n_{e.ped}$=7.6-8.1x10^{19} m^{-3}.

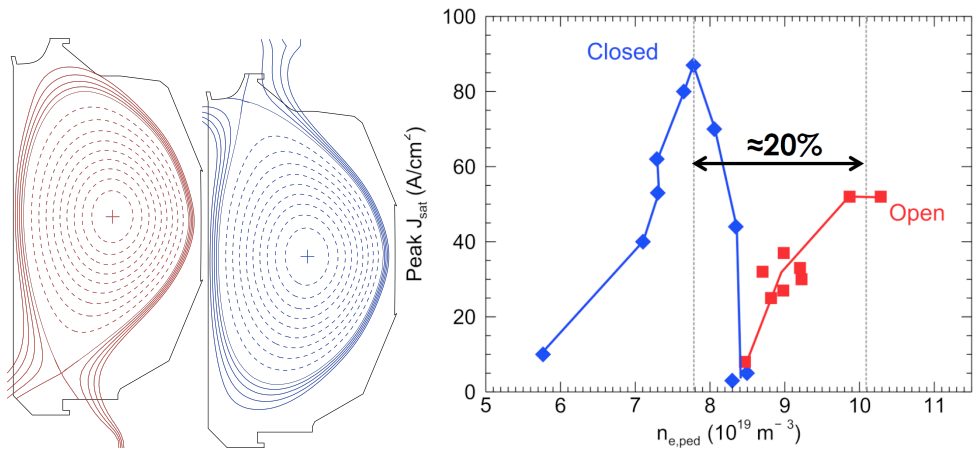

Figure 1: On the left: Open Lower Divertor (in red) and Closed Upper Divertor (in blue) magnetic equilibrium from EFIT. On the right: Peak J_{sat} at the target as function of $n_{e,ped}$ for open (red) and closed (blue) divertor. The roll over indicates the detachment onset.

Tangential filtered visible light cameras deliver C-III emission in both the lower and upper divertor. Carbon emission can be used to track the location of the temperature front which is a sharp function of the electron temperature. Tangential camera in the upper divertor indicated that the CIII emission shifts from the target for $n_{e,ped}$< 7.5x$10^{19}$$m^{-3}$ to up to the divertor leg for $n_{e,ped}$ >7.5x10^{19} m^{-3} indicating divertor detachment (not shown here). C-III emission from tangential camera at λ=465 nm for the open and closed configuration is displayed in Figure 2. Figure 2 shows that, for a given separatrix density chosen from the density scan, the open lower divertor strongly radiates at the outer strike point indicating attached conditions. In contrast, the detachment front in the closed upper divertor is peeling away from the target indicating the onset of detachment. Hence, these measurements also confirm that detachment occurs at lower upstream density for the closed divertor.

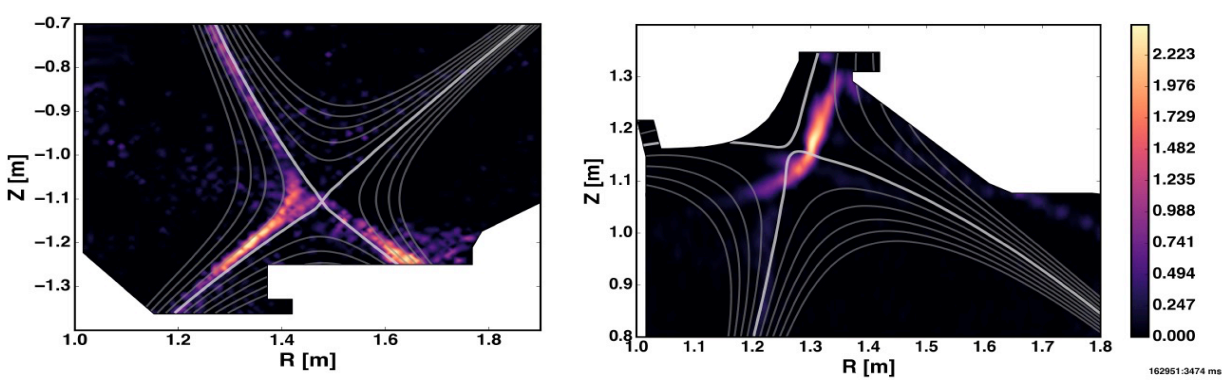

Figure 2 C-III emission can be used to track the detachment front location: while the open divertor radiates strongly at the outer strike point, in the closed divertor the detachment front drifts away from the target indicating detachment conditions.

Figure 3 show the experimental upstream n_e and T_e profiles measured by the Thomson scattering diagnostic for the open and closed divertors corresponding to the target conditions displayed in Figure 2. The plots show that approaching detachment, the closed divertor exhibits lower pedestal densities but higher pedestal temperatures compared to the open divertor. In addition we note that the density profile is shifted inward which can have consequences for the pedestal stability. The lower pedestal density observed in the closed divertor is the consequence of the fact that the closed configuration traps more neutrals into the divertor as will be shown in Section 4. On one hand this leads to greater power dissipation facilitating detachment (Section 4), and on the other hand, this means that less particle source is available to build the pedestal leading to lower pedestal fueling. The effect of divertor closure on plasma fueling and pedestal structure are still under investigation and are outside the scope of this work. In this work we investigastigate the closure's effects on power dissipation and detachment at the divertor targets.

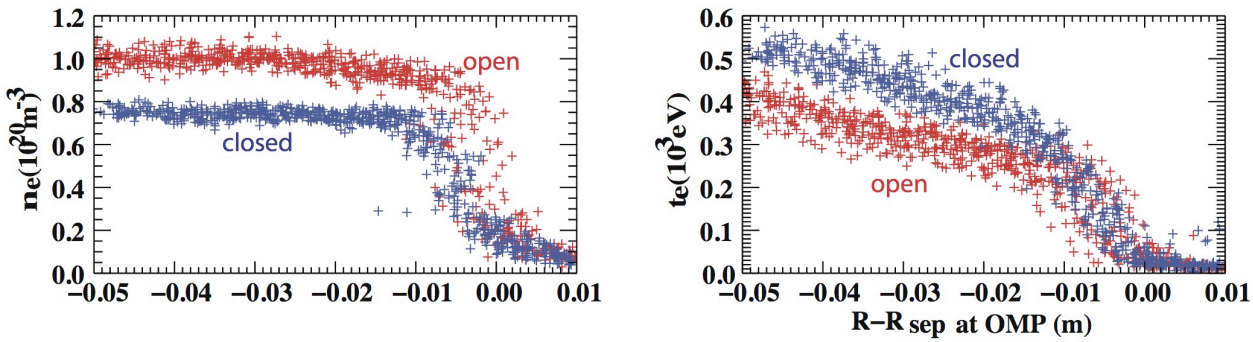

Figure 3: Experimental upstream profiles from core Thomson Scattering of n_e on the left and T_e on the right for open (in red) and closed (in blue) divertors.

3. **Modelling Setup**

The two DIII-D magnetic configurations are modeled by EFIT [7] . The computational meshes in the open LSN and closed USN cases, shown in Fig. 4, have the same span and resolution. All input parameters for LSN and USN cases are identical in order to allow a direct comparison between the two geometries and isolate the closure effects. Modeling was performed with SOLPS5.0, where the multi-fluid plasma transport code B2.5 [8] is coupled to the Eirene Monte Carlo neutral transport code [9]. B2.5 provides the plasma background on which the neutral trajectories are computed, and the associated particle, momentum, and energy sources for the fluid equations are deduced from Eirene. SOLPS is used in an interpretative way, meaning that the model transport coefficients are adjusted to match the measured upstream experimental profiles.

In these simulations the power at the core boundary is set to 2.8 MW equally divided between electrons and ions. To control the particle content in the simulations, a fixed core ion density at the innermost boundary is specified. The simulations include atomic processes relevant for detachment studies, such as elastic collisions and molecular assisted processes, but do not take drifts into account. Fortunately, it has been shown that drifts do not appreciably change the value of $n_{e,sep}$ at the onset of detachment, i.e, by more than 10% in DIII-D [10] [11]. At the target, sheath conditions are applied according to the standard Bohm criterion. Leakage type boundary conditions are used at the SOL and PFR, with the ion leakage in the outer boundary given by $\Gamma_{loss}= \alpha c_s n_\alpha$ (c_s: sound speed, n_ι: ion density, α: leakage factor, equal to 0.001). The missing ions will be transformed into neutral which are recycled back into the simulation domain. This compensation procedure depends on the recycling coefficient which in this work is set is set to be 100% for D. In addition to deuterium species (D^0, D_2, D^+, D_2^+) the simulations include carbon impurities from sputtering, using a constant chemical sputtering yield $Y_{chemical}$ = 0.01 for all material surfaces, while the physical sputtering-Y_{phys} is calculated using the modified Roth-Bohdansky formula [12]. Transport is classical in the parallel direction with ad-hoc user specified radial transport. In this work, the cross-field transport coefficients are chosen to reproduce the experimental upstream profiles. Inside the separatrix the anomalous diffusivities are D_{perp}= 0.8 m^2/s and x_{perp}= 1.5 m^2/s. Their values drop in the pedestal to 0.1 m^2/s to reproduce the features of the H-mode transport barrier and then they increase to 1 m^2/s in the SOL. Since we are interested in assessing changes in the divertor power dissipation due to the different geometries, the modelling for the closed configuration has been carried out using the same input parameters including the transport coefficients of the open divertor. This enable to

isolate the closure effect for given upstream conditions (Figure 4, right) and compare target performances in the two different geometries.

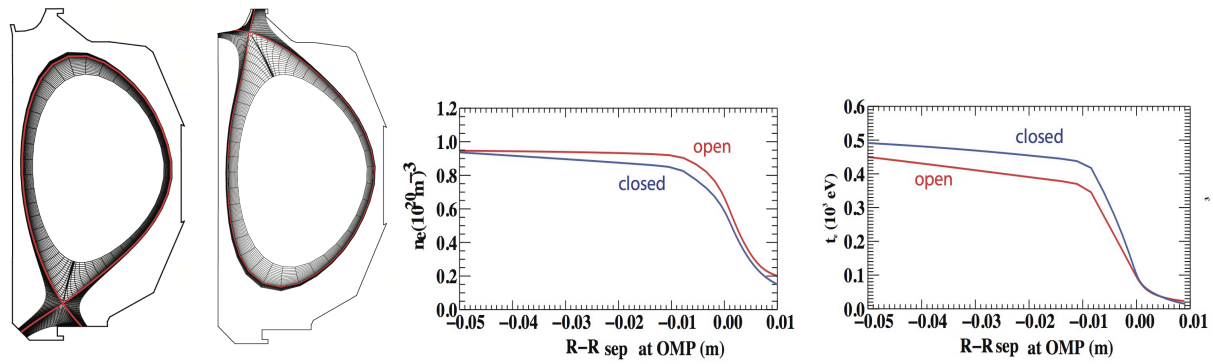

Figure 4: On the left: Meshes for the open lower divertor (left) and for the closed upper divertor (right). The separatrix position is shown in red. On the right: Upstream profiles of n_e and T_e in SOLPS.

4. Simulation results

Density scans for both open LSN and closed USN divertors have been carried out to investigate the density threshold for the transition to detachment. Figure 6 show heat flux and electron temperature as function of the midplane separatrix density $n_{e,sep}$. As $n_{e,sep}$ increases, the target power load is reduced as more power is exhausted before reaching the target. More in details, the reduction of q_{dep} is due to the combination of impurity radiation and volumetric recombination which decreases the energy available for ionization since more power is exhausted by radiation and collisional processes before reaching the target.
The density scan highlights that both the peak values (Figure 5, top) and the outer strike point (OSP) values (Figure 5, bottom) for T_e and q_{dep} are lower for the closed divertor at all densities. The closed divertor requires roughly a factor of 2 less in upstream density compared to the open divertor for T_e to drop below 2 eV. Hence, the more closed divertor detaches at a significantly lower upstream density than the open divertor. These results are in agreement with the experiments although in the latter the detachment threshold between the two configurations is less than the simulations suggest. Note that power loads at the targets are further reduced with increased density, due to increased volumetric losses.

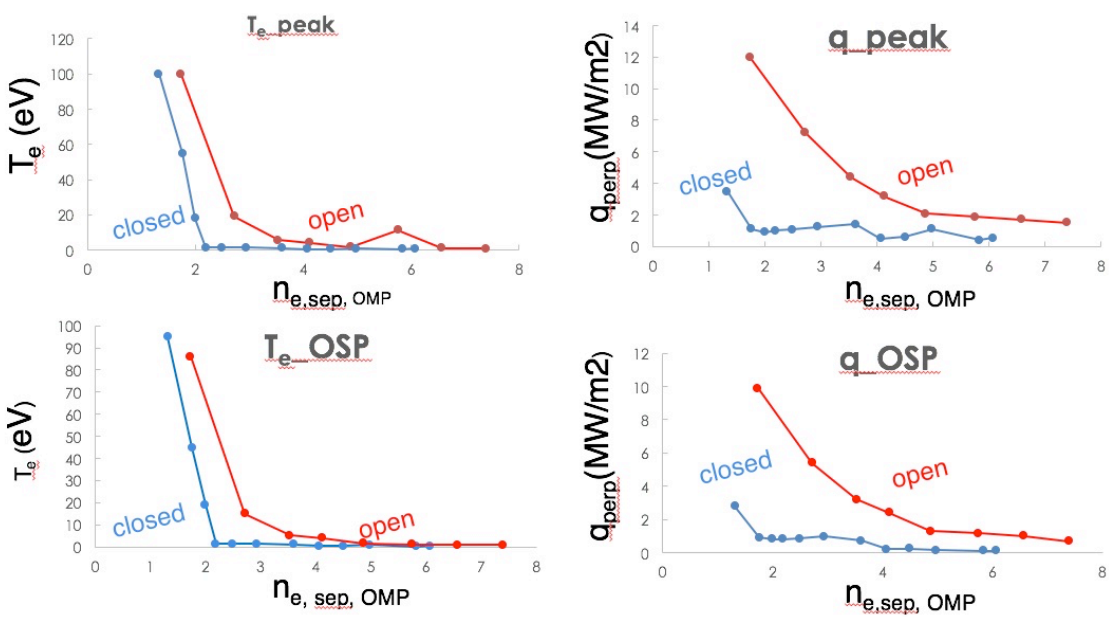

Figure 5: Density scan of T_e and q_{dep} for peak values (top) and OSP values (bottom) for the closed (blue) and open (red) divertor.

In the following, the effect of divertor closure is assessed by studying the distribution of the neutrals (and ionization sources). Figure 6 shows 2D contour plots of the molecular density, the electron temperature and the recycling source for both the open LSN (Figure 6, bottom) and the closed USN (Figure 6, top) configurations at a given separatrix density $n_{e,sep.}$ In the closed divertor, there is a strong build-up of the molecular density which does not take place in the open divertor. The high molecular density correlates with lower electron temperature. Cold temperatures between 1-2 eV are achieved at the strike point and along the whole target in the closed divertor, whereas the open divertor shows much higher temperatures at the strike point. The ionization front is drifting away in the closed divertor indicating the onset of detachment, whereas the open divertor has its detachment front at the strike point indicating that, for the same separatrix density, the open divertor is still attached. This is in qualitatively agreement with the experimental results reported in Section 2. The important correlation between high D_2 and low T_e indicated by SOLPS can be explained as follow: in the closed configuration, the molecules are trapped by the baffling and the higher neutral pressure enhances plasma-neutral collisions. The latter increase radiative and CX losses leading to a reduction of T_e and q_{dep}, where q_{dep} is the power deposited at the target. The reduction of T_e and q_{dep} due to neutral trapping facilitates greater divertor cooling, enabling the closed divertor to detach at lower upstream density than the open divertor, as shown also in the density scan (Figure 5).

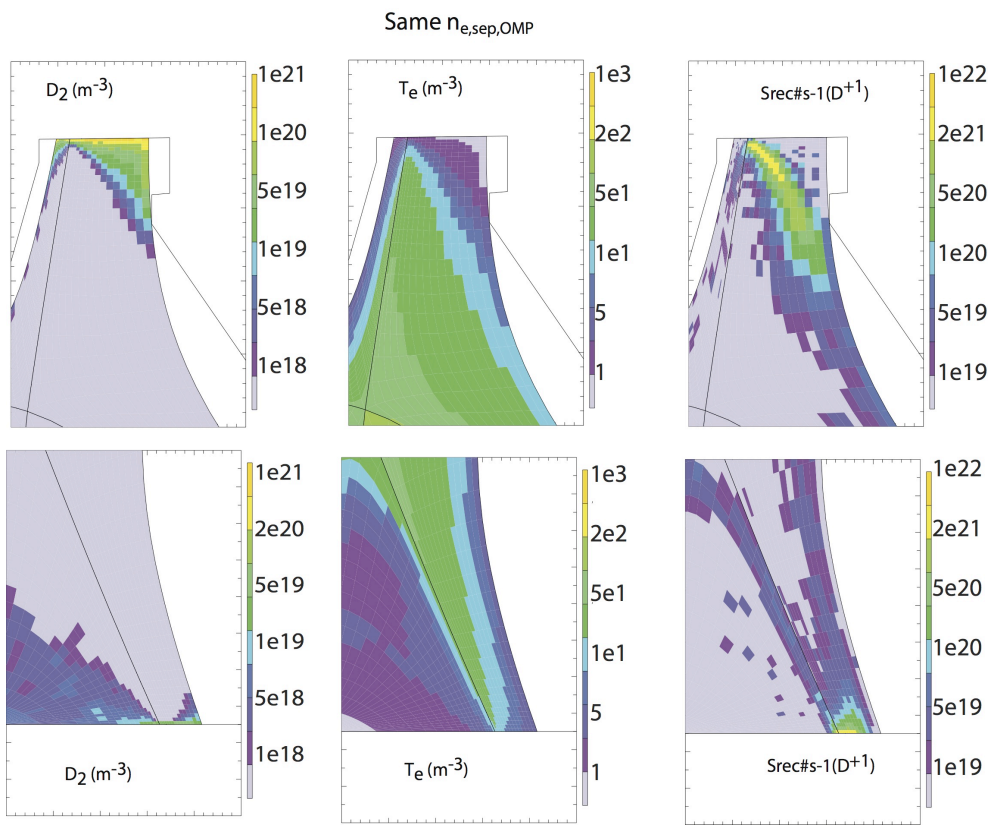

Figure 6:2D contour plots of molecular density D_2, T_e and ionization front for the closed (top) and open (bottom) divertors.

Finally, since we seek solutions to remove power load before it reaches the target, we analyze the effect of the power losses in the two different configurations. Figure 7 (left) shows the total losses for both configurations which are calculated as the total energy plasma loss due to impurity radiation and plasma-neutral collisions (neutral radiation, charge exchange and ionization processes). Figure 7 indicates that the closed divertor exhibits higher power losses than the open configuration consistent with the fact that the baffling of the closed divertor traps more neutrals which increases plasma-neutral collision and thus leading to enhanced power losses. To evaluate the effect of impurity radiation in the two cases, we break the total losses into the deuterium and carbon components. Figure 7 (right) indicates that at low n_e, C and D contribute equally to the power losses, but at higher n_e C radiation doubles compared to the losses given by D. This is due to the fact that as the density increases, carbon becomes less hot reaching the temperature region where it radiates more efficiently through the line components at low T_e as shown in figure 8. The black curve in Figure 8 is the radiative efficiency of carbon as function of T_e from the ADAS database. The plot shows that as the temperature decreases, the radiative efficiency of carbon increases till it reaches its maximum around 3 eV. Note that at temperatures between 1-2 eV its radiative efficiency remains still high. This means that C radiation is beneficial since it reduces the power flux and T_e to the point where the hydrogenic losses become important. Note that in absence of carbon, i.e. in metal machines, the role of carbon in reducing the power losses can be replaced by nitrogen seeding [13] [14].

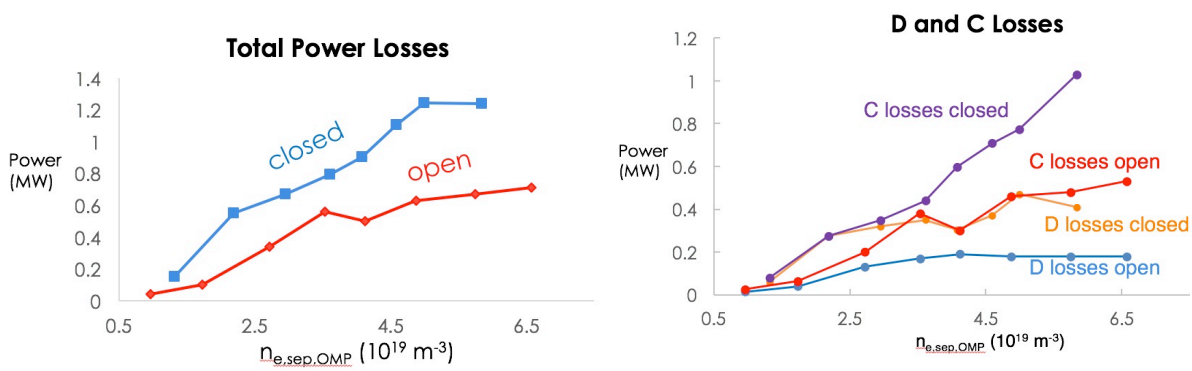

Figure 7: Total power losses in blue for closed divertor and in red for open divertor. On the right: C losses (violet) and D losses (orange) for the closed divertor, C losses (red) and D losses (blue) for the open divertor.

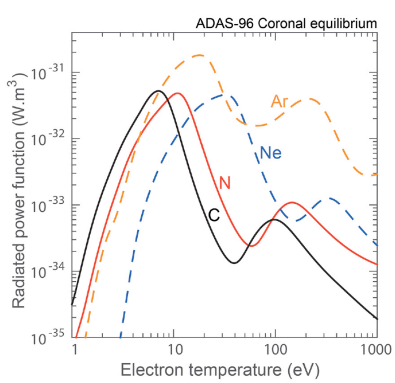

Figure 8: Radiative efficiency for impurities as function of Te. In black Lz curve from Carbon.

5. Conclusion

SOLPS modelling has been used for a detailed comparative study of the open vs closed divertor in the DIII-D tokamak in order to assess the impact of divertor's closure on plasma parameters and divertor conditions.

Although it is known that SOL transport codes encounter issues in reproducing quantitatively experimental measurements especially near detachment conditions, they are powerful tools for comparative studies and they can reveal important trends as the recycling behavior
discussed in this paper. Simulations of the closed and open divertor experiments have been carried out using the same input parameters and matching the experimental upstream profiles. This enables direct comparison of target conditions for the two different geometries and isolate the closure's effects. Modelling results show that the closed divertor achieve higher neutral densities than the open divertor. Higher atomic and molecular densities enhance plasma-neutral collisions, increasing radiative and CX losses which decrease T_e and the heat flux at the target. Power loads at the targets are further reduced with increased collisionality due to increased volumetric losses. Carbon impurity radiation plays an important role in the detachment process by reducing the temperature to the point where the hydrogenic losses become important without the need for additional low-Z impurity gas puffing. The enhancement of energy losses via controlling the recycling neutrals lead the closed upper divertor to detach at lower upstream density than the open lower divertor in qualitative agreement with the experimental observations.

The author thanks Aaro Jarvinen for support and fruitful discussions. *Work supported in part by the US Department of Energy under DE-AC05-06OR23100 and DE-FC02-04ER54698.

References

[1] P.C. Stangeby et al. "Obtaining reactor-relevant divertor conditions in tokamaks", *Nucl. Fusion* **51**, 063001 (2011)

[2] A. Loarte "Effects of divertor geometry on tokamak plasmas", *Plasma Phys. Control Fusion* **43**, R183-224 (2001)

[3] R. Neu et al. "The ASDEX Upgrade divertor IIb—a closed divertor for strongly shaped plasmas", *Nucl. Fusion* **43** 1191–6 (2003)

[4] B. Lipschultz et al."Variation of the divertor geometry in Alcator C-mod", *The 16th international conference on Fusion Energy"* p 425 (1996)

[5] A. Moser et al. "Effect of divertor closure on pedestal fueling and divertor detachment onset in DIII-D", *22nd International Conference on Plasma Surface Interactions (2016)*

[6] R. Schneider "Plasma Edge Physics with B2-Eirene", *Contrib. to Plasma Phys.* **4** 63–191 (2006)

[7] L. Lao et al. "Reconstruction of current profile parameters and plasma shape in tokamaks", *Nucl. Fusion* **25** 1611 (1985)

[8] B. J. Braams, "A multi-fluid code for simulation of the edge plasma in tokamaks", *Next European Torus (NET) report,* EUR-FU/XII-80/87/68, January (1987)

[9] D. Reiter "*The EIRENE Code User Manual"* (http://www.eirene.de/) (2009)

[10] A. McLean et al. " Drift-driven divertor asymmetries in the transition from attached to fully detached conditions", *57th Annual Meeting of the American Physical Society Division of Plasma Physics" (2015)*

[11] A. Jaervinen et al. "Interpretations of the impact of cross-field drifts on divertor flows in DIII-D with UEDGE", *22nd International Conference on Plasma Surface Interactions* , Rome (2016)

[12] J. Bohdansky and J. Roth "An analytic formula and important parameters for low-energy ion sputtering", *Journal of Applied Physics* **51**, 2861 (1980)

[13] A. Kallenbach et al. ”Impurity seeding for tokamak power exhaust: from present devices via ITER to DEMO”, *PPCF* **55** (2013), 124041

[14] M. Beurskens et al, “The effect of a metal wall on confinement in JET and ASDEX Upgrade”, PPCF, **55** (2013), 124043